

Supplementary Information

Reconstitution of [Fe]-hydrogenase using model complexes

Seigo Shima^{1,2,*}, Dafa Chen³, Tao Xu⁴, Matthew D. Wodrich^{4,5}, Takashi Fujishiro¹, Katherine M. Schultz⁴, Jörg Kahnt¹, Kenichi Ataka⁶ & Xile Hu^{4,*}

¹Max Planck Institute for Terrestrial Microbiology, 35043 Marburg, Germany.

²PRESTO, Japan Science and Technology Agency (JST), 332-0012 Saitama, Japan.

³School of Chemical Engineering and Technology, Harbin Institute of Technology, 150001 Harbin, China.

⁴Laboratory of Inorganic Synthesis and Catalysis, Institute of Chemical Science and Engineering, Ecole Polytechnique Fédérale de Lausanne (EPFL), 1015 Lausanne, Switzerland.

⁵Laboratory for Computational Molecular Design, Institute of Chemical Science and Engineering, Ecole Polytechnique Fédérale de Lausanne (EPFL), 1015 Lausanne, Switzerland.

⁶Department of Physics, Freie Universität Berlin, 14195 Berlin, Germany.

Index

Supplementary Methods.....	3
Chemicals.....	3
Enzyme activity assay.....	3
Phosphodiesterase digestion of the FeGP cofactor.....	4
Supplementary References.....	5
Supplementary Figure 1 Computed Energies for Hydrogen Binding and Activation by Model Complexes 1 and 2.	6
Supplementary Figure 2 Dependence of the [Fe]-hydrogenase activities on the substrate concentrations.....	7
Supplementary Figure 3 Dependence of activity of the forward reaction of the reconstituted [Fe]-hydrogenases on the H ₂ concentration in the assay buffer.....	8
Supplementary Figure 4 Effect of pH of the assay solutions on the activity of the reverse reaction.....	9
Supplementary Figure 5 Effects of GMP and pH on the activity of the [Fe]-hydrogenase holoenzyme reconstituted with the model complex 3i.....	10
Supplementary Figure 6 Effect of incubation time on the reconstitution of [Fe]-hydrogenase reconstituted with the model complex 3i.	11
Supplementary Figure 7 Possible reaction pathways for heterolytic H ₂ cleavage by model complex 5.....	12
Supplementary Figure 8 Possible reaction pathways for heterolytic H ₂ cleavage by model complex 6.....	13
Supplementary Figure 9 Change of UV-Vis spectrum of the FeGP cofactor by digestion with phosphodiesterase I.	14
Supplementary Figure 10 Mass of the light-decomposed product of the FeGP cofactor digested with phosphodiesterase I.....	15
Supplementary Figure 11 IR spectrum of [Fe]-hydrogenase reconstituted with the FeGP cofactor digested with phosphodiesterase.....	16
Supplementary Figure 12 Interactions of the Fe complex with the protein in the [Fe]-hydrogenase reconstituted with the native FeGP cofactor.	17
Supplementary Table 1 Occupancy of the model complex in the reconstituted [Fe]-hydrogenase.....	18
Supplementary Table 2 Reaction step free energies for different hydrogenase models....	19
Supplementary Table 3 Relative free energies (to structure A) of different species.....	20
Supplementary Table 4 Electronic energies, free energy corrections and COSMO-RS solvation energies (in THF) of relevant structures on the catalytic cycles for biomimics 2, 5 and 6.	21

Supplementary methods

Chemicals. Tetrahydromethanopterin and methenyl-tetrahydromethanopterin were extracted and purified from *Methanothermobacter marburgensis* as previously described¹. Methylene-tetrahydromethanopterin was chemically synthesized from tetrahydromethanopterin². Fe(CO)₅ was purchased from Beijing Zhongsheng Huateng Technology Co., Ltd. and Acros (Switzerland). Other chemicals were purchased from Sigma-Aldrich. The iron-pyridinol model complexes were prepared as previously described^{3,4}.

Enzyme activity assay. Conversion of methenyl-tetrahydromethanopterin to methylene-tetrahydromethanopterin and the reverse reaction catalyzed by reconstituted [Fe]-hydrogenase was determined photometrically. For the assay of the forward reaction, 30 μM (final concentration) methenyl-tetrahydromethanopterin was added to a 0.7 ml solution of 120 mM potassium phosphate (pH 7.5) containing 1 mM EDTA under 1.0 × 10⁵ Pa 100% H₂ atmospheres or N₂/H₂ mixture at 40 °C. The reaction was started by adding 10 μl reconstituted [Fe]-hydrogenase solution with a Hamilton syringe. Reduction of methenyl-tetrahydromethanopterin was determined by measuring the decrease in the absorbance at 336 nm. For the reverse reaction, 20 μM (final concentration) methylene-tetrahydromethanopterin was added to a 0.7 ml solution of 120 mM potassium phosphate (pH 6.0) containing 1 mM EDTA under a 100% N₂ atmosphere (1.5 × 10⁵ Pa) at 40 °C. The reaction was started by adding 5–20 μl reconstituted [Fe]-hydrogenase solution. Oxidation of methylene-tetrahydromethanopterin was determined by measuring the increase in the absorbance at 336 nm. The activities were calculated using the extinction coefficient of methenyl-tetrahydromethanopterin (ϵ at 336 nm = 21.6 mM⁻¹cm⁻¹)⁵. For the kinetic measurements shown in Fig. 4, the absorbance was measured with an Ultrospec 1100pro spectrophotometer (GE Healthcare); the spectra were recorded on a Specode S600 diode-

array spectrophotometer (Jena Analytik). For the cases of the forward (30 μM methenyl- H_4MPT^+ as a substrate) and reverse reactions (30 μM methylene- H_4MPT as a substrate), 0.005 mg/ml reconstituted enzyme (final concentrations) was added to the 0.7 ml reaction mixture; the light path of the cuvette was 1 cm. The spectra were recorded every 30 s.

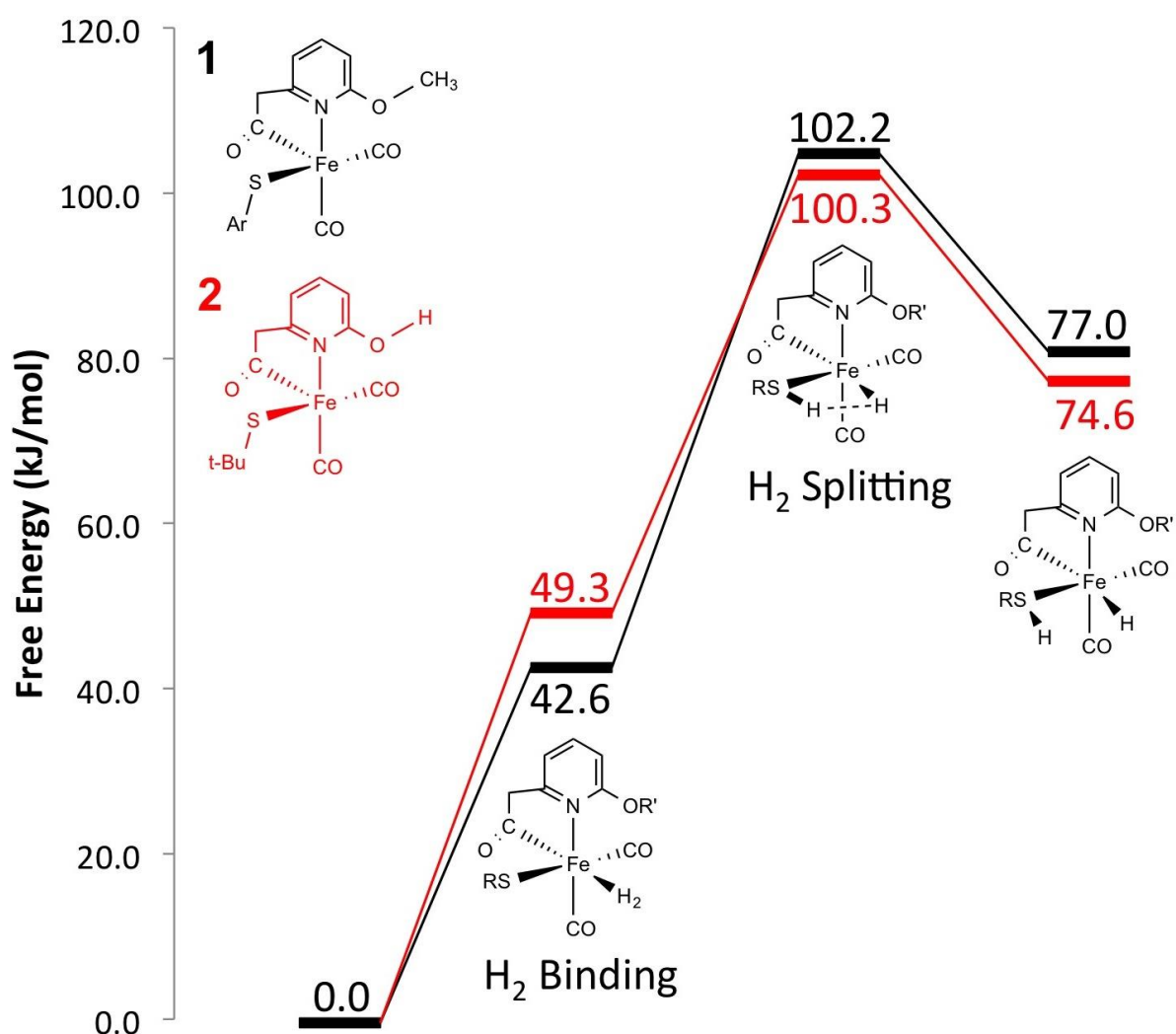
Production of H_2 upon oxidation of methylene-tetrahydromethanopterin was determined by gas chromatography. The 1 ml reaction mixture in 6 ml amber vials containing 120 mM potassium phosphate (pH 7.5), 250 μM methylene-tetrahydromethanopterin, and 2 mM GMP were preincubated at 40 $^\circ\text{C}$ for 5 min. The reaction was started by adding 4 μg of reconstituted [Fe]-hydrogenase. Aliquots (200 μl) of the gas phase were withdrawn with a gas-tight Hamilton syringe equipped with a Teflon valve and injected into a SRI 8610C gas chromatograph equipped with a 0.32 mm \times 1 m stainless-steel column with a molecular sieve (5 \AA , 80/100 mesh from Supelco) with helium as a carrier gas at 12 psi (8.3×10^4 Pa) (12.5 ml/min) at 80 $^\circ\text{C}$. H_2 was detected with a thermal conductivity detector. The H_2 concentration was calculated from the peak area at the retention time determined with a standard H_2 sample.

Phosphodiesterase digestion of the FeGP cofactor The FeGP cofactor was isolated from [Fe]-hydrogenase from *M. marburgensis* and separated from the protein by filtration as previously described.² The FeGP cofactor (0.2 mM final concentration) was digested with phosphodiesterase I from *Crotalus adamanteus* venom (USB) at 37 $^\circ\text{C}$ in a 100 mM glycine/NaOH pH 8.9 solution containing 100 mM NaCl, 15 mM MgCl_2 and 2-mercaptoethanol under N_2 . Progress of the digestion reaction was monitored with UV-Vis spectroscopy using a Specode S600 diodearray spectrophotometer (Analytik Jena). The [Fe]-hydrogenase was reconstituted with the phosphodiesterase-digested cofactor in a solution containing 0.1 mM apoenzyme, 0.14 mM digested FeGP cofactor, 100 mM citrate buffer pH

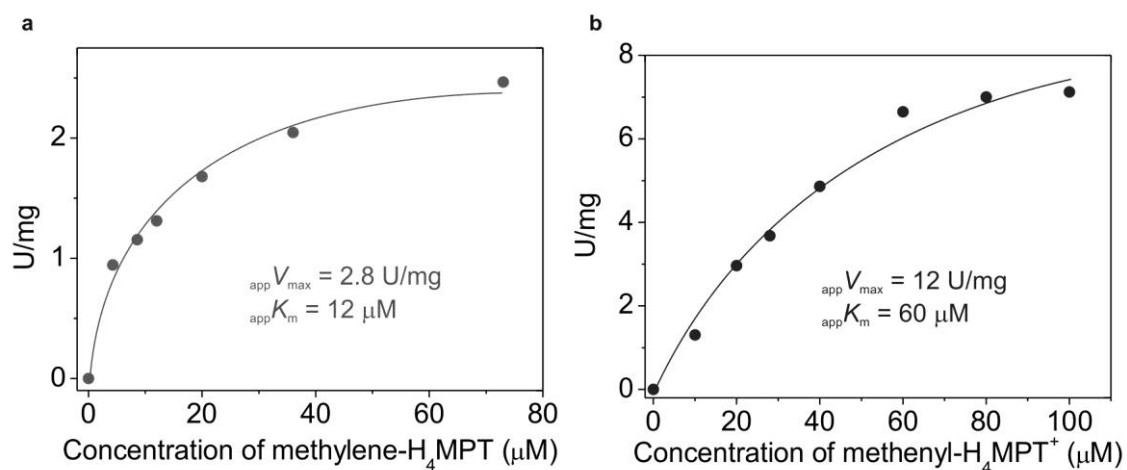
5.6 and 2 mM GMP. The solution was incubated on ice for at least 1 hour. Ten μ l of the reconstituted enzyme solution was assayed for the [Fe]-hydrogenase activity. The intact FeGP cofactor and the iron complex of the digested product could not be detected with Matrix-assisted laser desorption/ionization time-of-flight mass spectrometry (MALDI-TOF-MS). Therefore, to detect the phosphodiesterase-digestion products, an aliquot of the digested products were exposed to white light to decompose the iron complex to pyridinol compound and then analysed with MALDI-TOF-MS using a 4800 Proteomics Analyzer (Applied Biosystems/MDS SCIEX) and an α -cyano-4-hydroxycinnamic acid matrix.

Supplementary References

- 1 Shima, S. & Thauer, R. K. Tetrahydromethanopterin-specific enzymes from *Methanopyrus kandleri*. *Methods Enzymol.* 331, 317-353, (2001).
- 2 Shima, S., Schick, M. & Tamura, H. Preparation of [Fe]-hydrogenase from methanogenic archaea *Methods Enzymol* 494, 119-137, (2011).
- 3 Chen, D., Scopelliti, R. & Hu, X. A five-coordinate iron center in the active site of [Fe]-hydrogenase: hints from a model study. *Angew. Chem. Int. Ed.* 50, 5671-5673, (2011).
- 4 Hu, B., Chen, D. & Hu, X. Synthesis and reactivity of mononuclear iron models of [Fe]-hydrogenase that contain an acylmethylpyridinol ligand. *Chem. Eur. J.* 20, 1677-1682, (2014).
- 5 DiMarco, A. A., Bobik, T. A. & Wolfe, R. S. Unusual coenzymes of methanogenesis. *Annu. Rev. Biochem.* 59, 355-394, (1990).

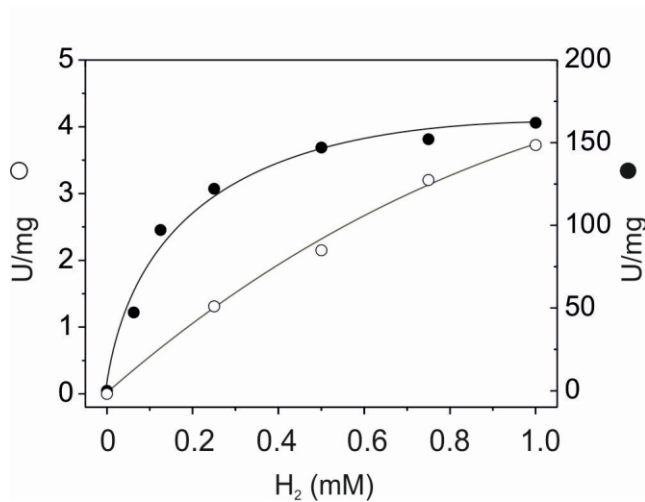


Supplementary Figure 1 | Computed Energies for Hydrogen Binding and Activation by Model Complexes 1 and 2. Computations at the B3LYP-dDsC/TZ2P//M06/def2-SVP level including free energy corrections at the M06/def2-SVP level and solvation corrections (in implicit) THF using the COSMO-RS solvation model.

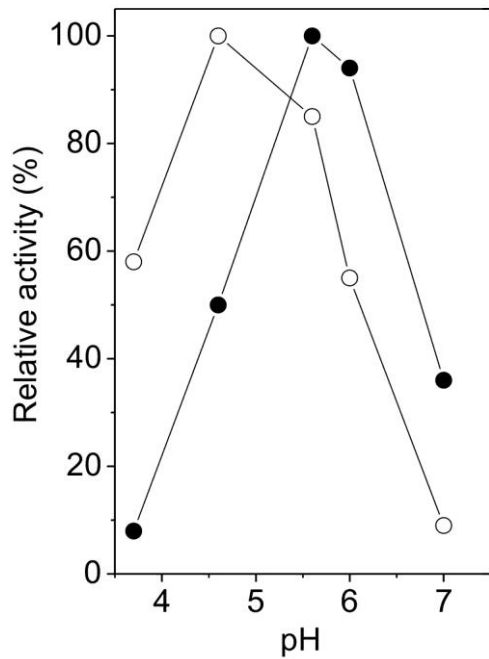


Supplementary Figure 2 | Dependence of the [Fe]-hydrogenase activities on the substrate

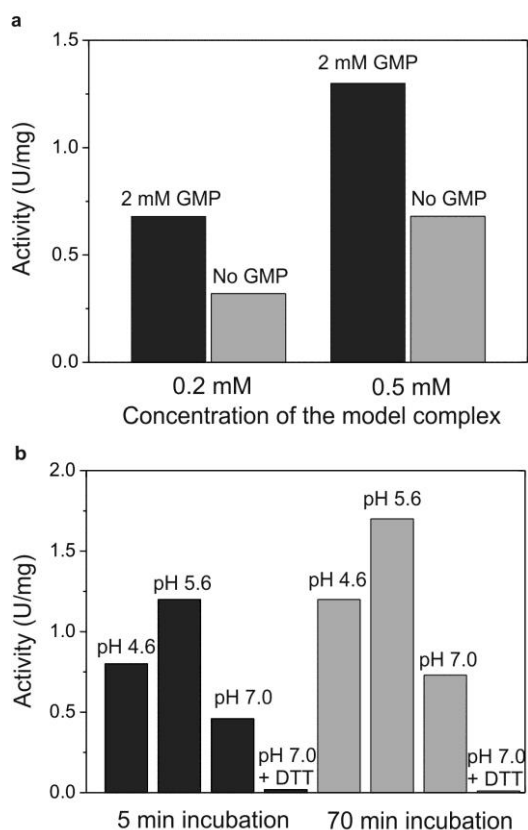
concentrations. a, Activity of the reverse reaction and **b**, activity of the forward reaction of the [Fe]-hydrogenase reconstituted with **3i** were tested in standard assay conditions at 40°C. The apparent V_{max} and apparent K_m values were calculated using curve-fitting. The apparent K_m values for methenyl- H₄MPT⁺ and methylene-H₄MPT of the wild-type enzyme are 10 μM and 20 μM, respectively.



Supplementary Figure 3 | Dependence of activity of the forward reaction of the reconstituted [Fe]-hydrogenases on the H₂ concentration in the assay buffer. [Fe]-hydrogenase reconstituted with **3i** (open circles) and with the FeGP cofactor (closed circles) were tested in the standard assay under the gas phase containing different H₂ concentration. The apparent V_{\max} and apparent K_m values were calculated using curve-fitting. The H₂ concentration in the assay solution (shown in abscissa) was calculated from the H₂ concentration in the gas phase; 100% H₂ (approximately 10⁵ Pa) in the gas phase corresponds to approximately 1 mM in the assay solutions. The apparent V_{\max} and apparent K_m of the enzyme reconstituted with the FeGP cofactor is 180 U/mg and 0.1 mM, respectively. The apparent K_m of the enzyme reconstituted with **3i** is greater than 1 mM (H₂) and its V_{\max} could be higher than 4 U/mg but it cannot be determined as K_m is too large.

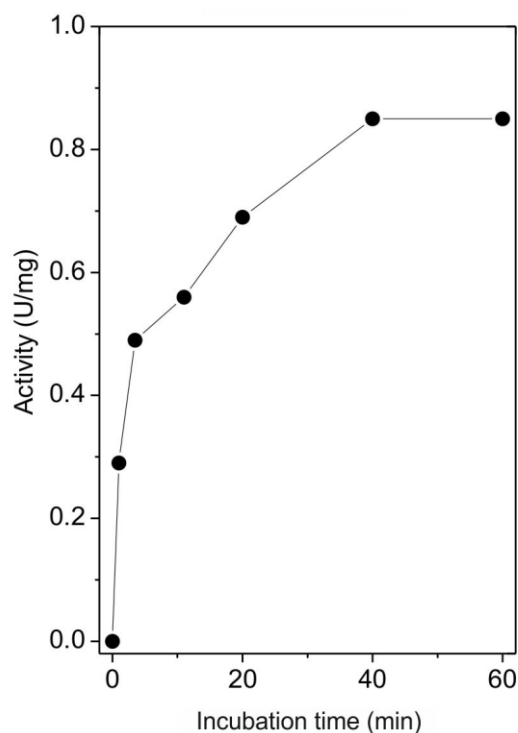


Supplementary Figure 4 | Effect of pH of the assay solutions on the activity of the reverse reaction. [Fe]-hydrogenase reconstituted with **3i** (open circles) and with the FeGP cofactor (closed circles) were tested in the standard assay conditions using 100 mM sodium acetate buffer pH 3.7, pH 4.6 and pH 5.6 as well as 120 mM potassium phosphate buffer pH 6.0 and 7.0. All buffers contained 1 mM EDTA.



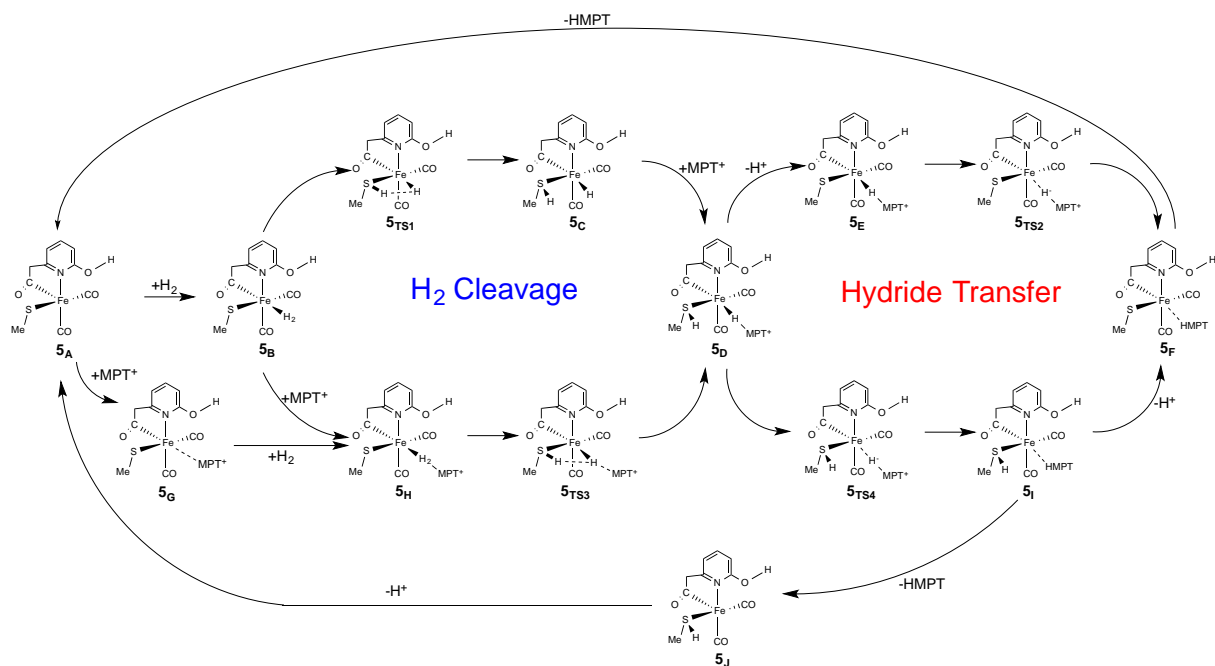
Supplementary Figure 5 | Effects of GMP and pH on the activity of the [Fe]-hydrogenase

holoenzyme reconstituted with the model complex 3i. **a**, Effect of GMP. The anoxic reconstitution mixture contained 35 mM Mops/KOH pH 7, 0.02 mM [Fe]-hydrogenase apoenzyme, and **3** at the concentrations indicated. The model complex **3** was dissolved in methanol containing 1% acetic acid and then added into the solution; the final pH of the reconstitution solution was around 5. The reconstitution mixture containing or lacking 2 mM GMP was incubated on ice for 1 h before the activity was measured. **b**, Effect of pH. The conditions for [Fe]-hydrogenase reconstitution were the same as those described in **a** except that the buffer solution was 50 mM sodium acetate buffer (pH 4.6), 50 mM sodium acetate buffer (pH 5.6), 50 mM Mops/KOH buffer (pH 7.0), or 50 mM Mops/KOH buffer (pH 7.0) plus 50 mM dithiothreitol (DTT). The reverse reaction was assayed photometrically.

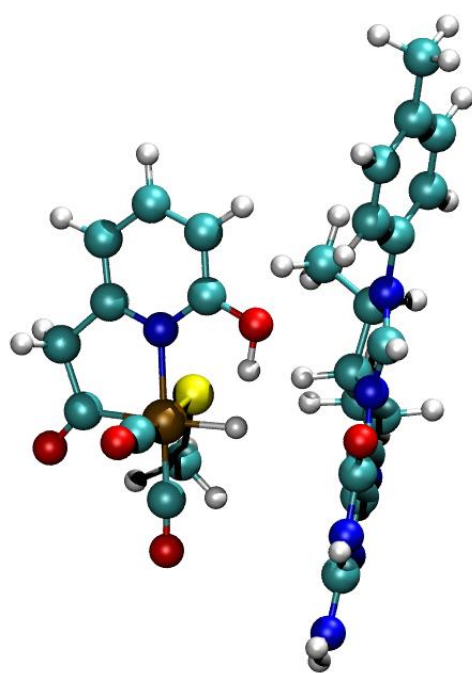
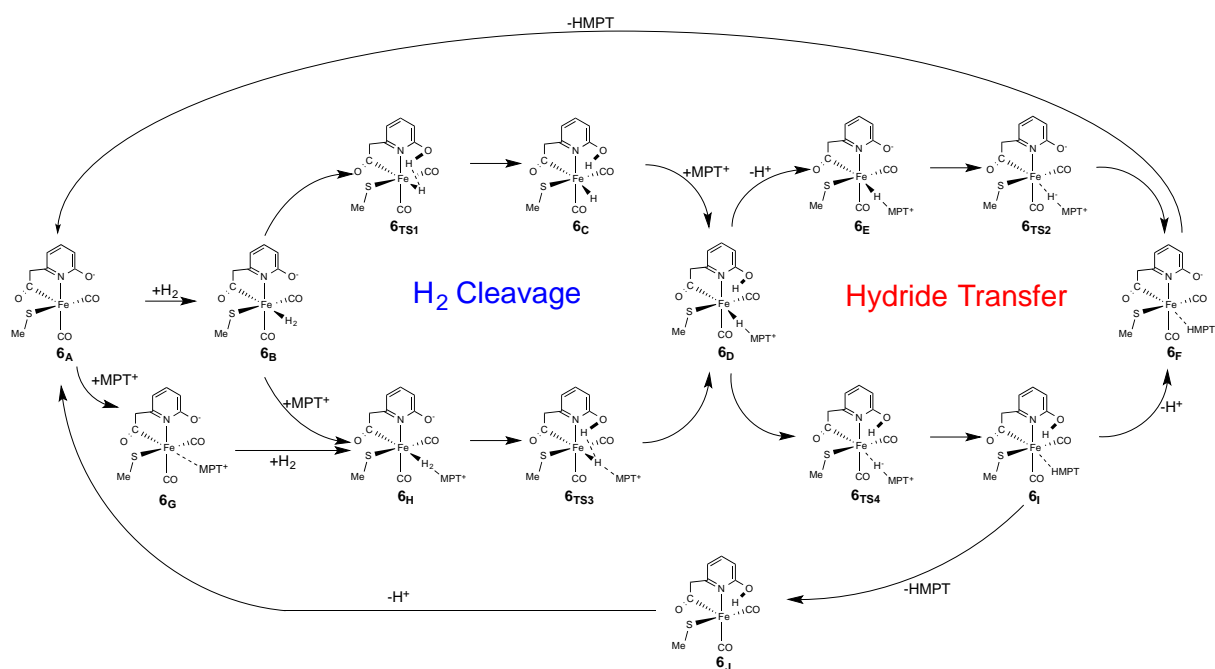


Supplementary Figure 6 | Effect of incubation time on the reconstitution of [Fe]-

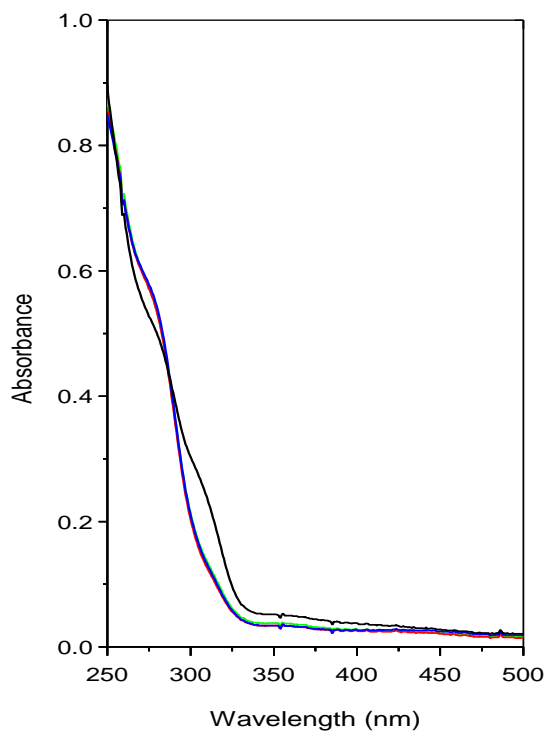
hydrogenase reconstituted with the model complex 3i. The model complex **3** dissolved in methanol containing 1% acetic acid was added into 100 mM sodium acetate buffer (pH 5.6), 2 mM GMP, and 0.02 mM [Fe]-hydrogenase apoenzyme; the mixture was thoroughly mixed by vortexing and then incubated on ice. Ten μ l of the reconstitution solution was withdrawn and mixed with the standard assay solution containing 20 μ M methylene-tetrahydromethanopterin at 40 °C under N₂. The concentration of the model complex was 0.2 mM.



Supplementary Figure 7 | Possible reaction pathways for heterolytic H₂ cleavage by model complex 5. A truncated MPT⁺ substrate was used as a hydride acceptor and 1-methylimidazole was used as a proton acceptor. The catalytic pathway involving 5B, 5TS1, 5C, 5TS4, and 5I is not indicated in Fig. 6 of the main text.

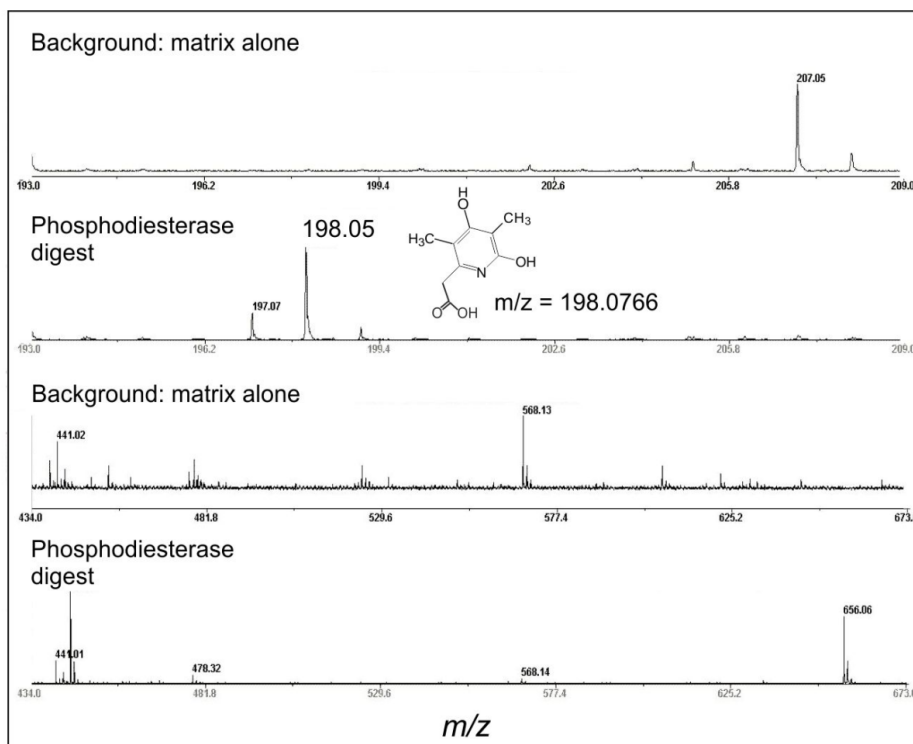


Supplementary Figure 8 | Possible reaction pathways for heterolytic H₂ cleavage by model complex 6. A truncated MPT⁺ substrate was used as a hydride acceptor and 1-methylimidazole was used as a proton acceptor. The catalytic pathway involving 6_B, 6_{TS1}, 6_C, 6_{TS4} and 6_I is not indicated in Fig. 6 of the main text. The structure of 6D is shown on the bottom.

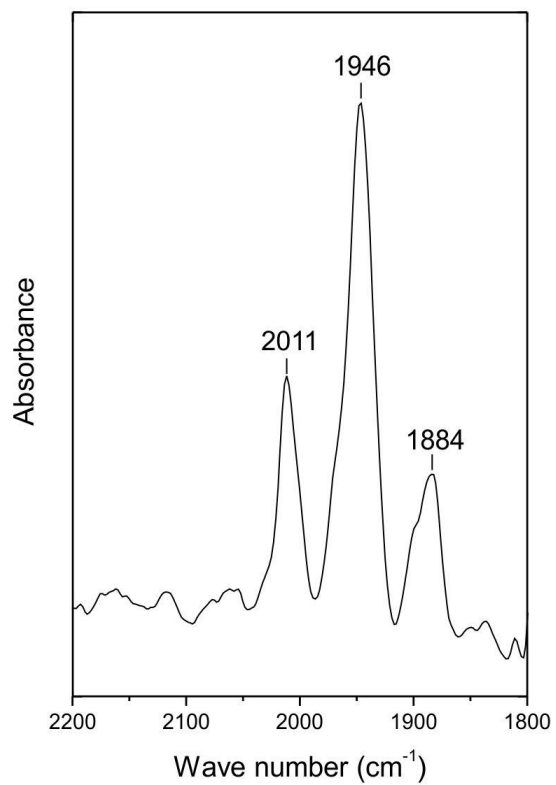


Supplementary Figure 9 | Change of UV-Vis spectrum of the FeGP cofactor by digestion

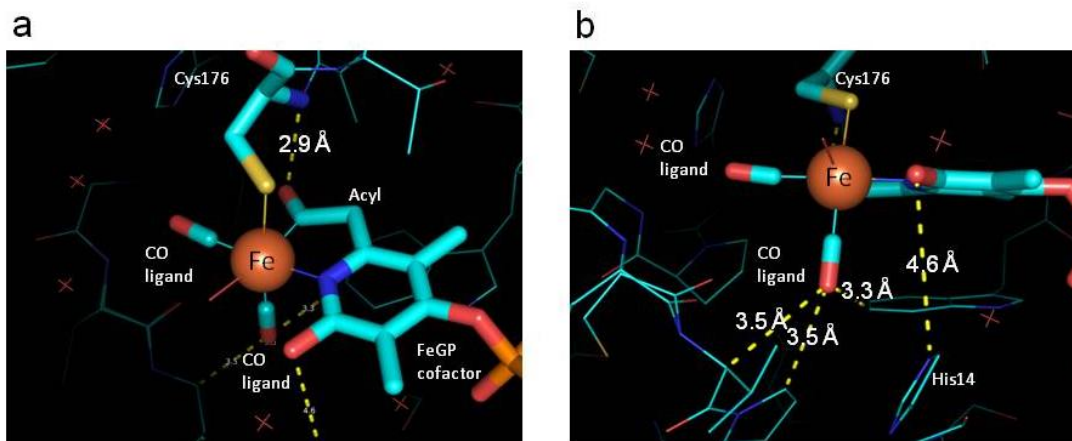
with phosphodiesterase I. The FeGP cofactor (0.2 mM) was digested with phosphodiesterase I from *Crotalus adamanteus* Venom (USB) at 37 °C in 100 mM glycine/NaOH (pH 8.9) containing 100 mM NaCl, 15 mM MgCl₂ and 2-mercaptoethanol. UV-Vis spectrum was measured by diode-array spectrophotometer Specode S600 (Jena Analytik) using a quartz cuvette (1-cm light pass), just after addition of 1 U/ml phosphodiesterase (black line) and after incubation for 10 min (green line), 20 min (red line) and 60 min (blue line). As the reaction was completed within 10 min in this assay condition, the three UV-Vis spectra of the after incubation overlap.



Supplementary Figure 10 | Mass of the light-decomposed product of the FeGP cofactor digested with phosphodiesterase I. The intact FeGP cofactor and the iron complex of the digested product cannot be detected by Matrix-assisted laser desorption/ionization time-of-flight mass spectrometry (MALDI-TOF-MS). Therefore, the digested products in the samples shown in Supplementary Fig. 9 were exposed to white light for decomposition and then analysed by MALDI-TOF-MS using a 4800 Proteomics Analyzer (Applied Biosystems/MDS SCIEX) and an α -cyano-4-hydroxycinnamic acid matrix. As background, a sample containing only the matrix was also measured. The theoretical light decomposed product of the digested cofactor, 6-carboxymethyl-3,5-dimethyl-4-hydroxy-2-pyridone ($m/z = 198$) was detected (Chemical structure is show in this figure). The m/z 198 peak was not detected in the background. The light-decomposed product of the intact FeGP cofactor, (6-carboxymethyl-3,5-dimethyl-2-pyridone-4-yl)-(5'-guanosyl) phosphate ($m/z = 543$) was not detected. This result indicates that the FeGP cofactor was completely digested by phosphodiesterase I in this condition.



Supplementary Figure 11 | IR spectrum of [Fe]-hydrogenase reconstituted with the FeGP cofactor digested with phosphodiesterase.



Supplementary Figure 12 | Interactions of the Fe complex with the protein in the [Fe]-hydrogenase reconstituted with the native FeGP cofactor. a. The acyl-oxygen is bound to the main-chain NH by a hydrogen-bond (2.9 Å). **b.** one of the CO ligands (trans to Cys-S) is fixed through multiple hydrophobic interactions (3.3-3.5 Å). The distance between the 2-hydroxy and the catalytically important His14 is 4.6 Å. The FeGP cofactor and the Cys176 side chain are shown with stick models. PDB code of the protein structure is 3F47. The cysteine-sulphur is covalently bound to the iron.

Supplementary Table 1 | Occupancy of the model complex in the reconstituted [Fe]-

hydrogenase. The occupancy was calculated from the ratio of areas of the two CO peaks of the complex and the amide II peak of the protein in the IR spectra.

Reconstituted enzyme	(A) CO peak 1 area	(B) CO peak 2area	(C) Total CO peak area (A + B)	(D) Amide II peak area	(E) CO/amide II ratio (C/D)	(F) Occupancy (E/0.0064) ¹
Wild FeGP	0.18	0.16	0.34	53	0.0064	1.0
Wild 3i -GMP	0.25	0.43	0.68	57	0.012	1.9
Wild 3i +GMP	0.082	0.052	0.13	37	0.0035	0.55
Wild 4i -GMP	0.032	0.026	0.058	20	0.0029	0.45
Wild 4i +GMP	0.048	0.042	0.090	30	0.0030	0.47
C176A FeGP	0.15	0.15	0.3	47	0.0063	0.98
C176A 3i -GMP	0.21	0.43	0.64	50	0.013	2.0
C176A 3i +GMP	0.12	0.45	0.57	60	0.0095	1.5
Wild enzyme digested FeGP	0.011	0.001	0.012	45	0.00027	0.04

¹Occupancy of the FeGP cofactor was calculated based on the CO/amide II peak-area ratio of native [Fe]-hydrogenase purified from *Methanothermobacter marburgensis*.

Supplementary Table 2 | Reaction step free energies for different hydrogenase models.

Computations at the B3LYP-dDsC/TZ2P//M06/def2-SVP level including free energy corrections at the M06/def2-SVP level and solvation corrections (in implicit) THF using the COSMO-RS solvation model. Values in kJ/mol.

Reaction	OH-SMe (5)	O-SMe (6)	OH-StBu
A → B	45.0	31.1	49.3
A → G	45.2	8.1	--
B → TS1	64.3	2.4	52.9
B → H	51.9	10.3	--
TS1 → C	-37.1	-5.0	-25.2
C → D	24.8	12.7	--
D → TS4	32.8	39.0	--
D → F	--	-6.8	--
D → E	22.8	--	--
TS4 → I	-22.9	-64.6	--
I → F	-79.7	18.8	--
I → J	-12.5	-11.9	--
F → A	-23.8	-31.0	--
H → TS3	39.6	1.9	--
TS3 → D	-39.5	-2.2	--
E → TS2	8.0	--	--
TS2 → F	-100.7	--	--
J → A	-91.0	-0.4	--
G → H	51.7	33.4	--

Supplementary Table 3 | Relative free energies (to structure A) of different species.

Computations at the B3LYP-dDsC/TZ2P//M06/def2-SVP level including free energy corrections at the M06/def2-SVP level and solvation corrections (in implicit) THF using the COSMO-RS solvation model. Values in kJ/mol.

Species	OH-SMe (5)	O-SMe (6)^[a]	OH-StBu
A	0.0	15.3	0.0
B	45.0	46.4	49.3
C	72.2	43.8	77.0
D	97.0	56.5	--
E	119.8	--	--
F	27.1	49.6	--
G	45.2	23.4	--
H	96.9	56.7	--
I	106.8	30.8	--
J	94.3	19.0	--
TS1	109.3	48.8	102.2
TS2	127.8	--	--
TS3	136.5	58.6	--
TS4	129.7	95.5	--

[a] Energies relative to 5A.

Supplementary Table 4 | Electronic energies, free energy corrections and COSMO-RS solvation energies (in THF) of relevant structures on the catalytic cycles for biomimics 2, 5 and 6. Values in hartree.

Compound	M06/def2-SVP Electronic Energy	M06/def2-SVP Free Energy Correction	B3LYP-dDsC/TZ2P Electronic Energy	B3LYP-dDsC Solvation Correction
H ₂	-1.166462	-0.001451	-0.283657	0.001243
MPT ⁺	-1062.643192	0.321973	-11.919487	-0.102494
HMPT	-1063.369283	0.332296	-12.259383	-0.046135
1-methylimidazole	-265.154660	0.068916	-3.123859	-0.009742
1-methylimidazole-H ⁺	-265.607883	0.082835	-3.057470	-0.099413
2 _A	-2520.534459	0.210091	-9.431548	-0.036338
2 _B	-2521.700533	0.226532	-9.712542	-0.036877
2 _C	-2521.687023	0.227032	-9.701585	-0.037774
2 _{TS1}	-2521.676358	0.223260	-9.689900	-0.036106
5 _A	-2402.770155	0.130972	-7.369282	-0.034423
5 _B	-2403.939235	0.147705	-7.652381	-0.034783
5 _C	-2403.923883	0.148747	-7.644007	-0.033845
5 _D	-3466.583682	0.495243	-19.594083	-0.120828
5 _E	-3466.113586	0.484939	-19.594009	-0.092543
5 _F	-3466.170800	0.490313	-19.664113	-0.063102
5 _G	-3465.441522	0.484728	-19.319858	-0.120409
5 _H	-3466.592769	0.498283	-19.586610	-0.131384
5 _I	-3466.603028	0.501353	-19.613480	-0.103782
5 _J	-2403.194539	0.141223	-7.292550	-0.096122
5 _{TS1}	-2403.910704	0.145462	-7.626953	-0.033495
5 _{TS2}	-3466.117797	0.485542	-19.603182	-0.080910
5 _{TS3}	-3466.569950	0.492561	-19.572306	-0.124876
5 _{TS4}	-3466.572793	0.494642	-19.587786	-0.114050
6 _A	-2402.296549	0.118899	-7.302355	-0.074104
6 _B	-2403.469776	0.135731	-7.592984	-0.072308
6 _C	-2403.470793	0.137892	-7.592458	-0.075989
6 _D	-3466.143196	0.482737	-19.631359	-0.077119
6 _F	-3465.680880	0.476630	-19.583314	-0.112301
6 _G	-3464.975378	0.466796	-19.349905	-0.071369
6 _H	-3466.145780	0.485034	-19.636029	-0.074643
6 _I	-3466.172191	0.491768	-19.665751	-0.061509
6 _J	-2402.774895	0.132738	-7.378616	-0.020904
6 _{TS1}	-2403.464884	0.133892	-7.589537	-0.072994
6 _{TS3}	-3466.139781	0.480472	-19.630388	-0.074996
6 _{TS4}	-3466.134515	0.487661	-19.625741	-0.072790